Protein Perdeuteration

DOI: 10.1002/anie.201207071

Near-Atomic Resolution Neutron Crystallography on Perdeuterated *Pyrococcus furiosus* Rubredoxin: Implication of Hydronium Ions and Protonation State Equilibria in Redox Changes**

*M. G. Cuypers, S. A. Mason, M. P. Blakeley, E. P. Mitchell, M. Haertlein, and V. Trevor Forsyth**

Rubredoxins are small monomeric non-heme, mononuclear iron-sulfur cluster proteins found in prokaryotes[1] and in some eukaryotes.[2] Although a multitude of roles have been proposed,[3] the main functions of the rubredoxins remain uncertain. Rubredoxin from *Pyrococcus furiosus (Pf)* is one of the most thermostable proteins known, with a melting temperature of 200 °C, and it can resist denaturation over prolonged periods at temperatures of up to 95 °C.[4] The structure of the hyperthermophilic *Pf* rubredoxin does not contain an unusual number of hydrogen bonds but has a richly H-bonded N-terminus region involving residue Glu14, which is absent in mesophilic rubredoxins. It has been suggested that this may contribute to the high thermostability of *Pf* rubredoxin.[5] As a redox protein, rubredoxin is also an important model system for an understanding of electron transfer processes associated with catalysis. Iron–sulfur proteins occur widely, covering a wide range of redox potentials, and this variation may be attributable to variations in solvation, hydrogen bonding, and electrostatic interactions.

The aim of the current work was to obtain high-resolution neutron crystallographic information from both oxidized and reduced forms of perdeuterated *Pf* rubredoxin by fully exploiting the power of neutrons to clearly image water molecules, hydronium ions, and the protonation of carboxylic and hydroxylic moieties. Neutron diffraction is the only method that can provide this level of detail. The D19 instrument at the Institut Laue-Langevin (ILL) is a monochromatic diffractometer that allows atomic resolution studies of systems for which suitably large crystals are available. It complements the quasi-Laue instrument LADI-III, which has a much broader scope for neutron protein crystallography and which is capable of providing good results for systems having larger unit cells and smaller crystal volumes. The isotopic replacement of hydrogen by deuterium atoms allows their identification in neutron scattering density maps, with a visibility comparable to that of other elements in biological macromolecules, as well as helping to reduce the high experimental background due to the large incoherent scattering cross-section of hydrogen.[6] Perdeuterated protein was produced in the Deuteration Laboratory of ILL's Life Science Group; its use allows both the elimination of hydrogen incoherent scattering and also the enhancement of the visibility of deuterium by comparison with its lighter isotope hydrogen. The study was carried out to a resolution of 1.27 Å in the case of the oxidized form (PDB: 4AR3) and to 1.38 Å resolution for the reduced form (PDB: 4AR4). This is the first high-resolution neutron study of *Pf* rubredoxin in both forms. It reveals information beyond that attainable in previous lower-resolution studies of hydrogenated[7] and deuterated systems.[8] The combination of monochromatic neutron crystallography and protein perdeuteration has played a key role in obtaining this high-quality structural information.

Our neutron structural analysis is fully consistent with previous X-ray studies of both the reduced and oxidized structures of the protein. However, the availability of high-resolution neutron crystallographic data in the current work has led to several remarkable observations that are beyond the scope of X-ray studies. The ability to determine the locations, occupancies, and temperature factors of hydrogen atoms (present as deuterium in this study) has resulted in the observation of several hydronium ions that are clearly implicated in the stability of both redox forms of the protein. All of the features discussed here were checked carefully on the basis of consistency with $2F_0-F_c$, F_0-F_c and omit Fourier synthesis maps. An essential aspect of this work is the assumption that hydrogenated and perdeuterated forms of the protein are to a high degree isomorphous (RMSD between PDB 1VCX (H rubredoxin) and 4AR3 (D rubredoxin) over C-alpha atoms is 0.105 Å. Please note that D_3O^+ ions are referred to throughout as "hydronium" instead of the more correct but cumbersome description "deuterium-substituted hydronium".

The first deuterium-substituted hydronium (D_3O^+) ion (HYD1, Figure 1) is located near Leu51 and is present in both the reduced and oxidized forms. It was refined with all atoms

[*] Dr. M. G. Cuypers, Prof. E. P. Mitchell, Prof. V. T. Forsyth
EPSAM/ISTM, Keele University
Staffordshire, ST5 5BG (UK)
Dr. M. G. Cuypers, Dr. S. A. Mason, Dr. M. P. Blakeley, Dr. M. Haertlein, Prof. V. T. Forsyth
ILL
6, rue Jules Horowitz, 38042 Grenoble (France)
E-mail: tforsyth@ill.fr
Prof. E. P. Mitchell
ESRF, Grenoble (France)

[**] V.T.F. and S.A.M. acknowledge EPSRC support for the construction of the D19 diffractometer under grant GR/R47950/01 to Durham, Keele, and Bath Universities. V.T.F. also acknowledges EPSRC support under grant EP/C015452/1 and from the EU under contract RII3-CT-2003-505925. We thank the ILL for provision of neutron beamtime on D19, and the ESRF for time on beamline ID-29. We gratefully acknowledge J. B. Artero and M. Moulin for help with fermentation procedures.

Supporting information for this article is available on the WWW under http://dx.doi.org/10.1002/anie.201207071.

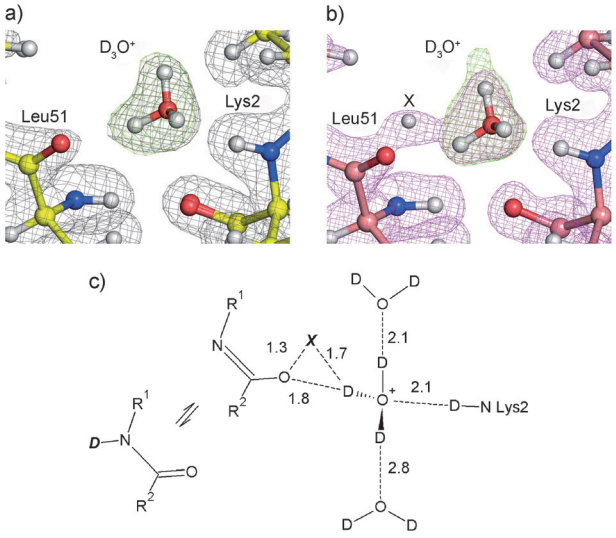

Figure 1. Neutron scattering density maps showing the HYD1 D_3O^+ ion located near Leu51 in both the reduced (a) and oxidized (b) forms of the protein. In each case, the $2F_0-F_c$ map (contoured at 1σ, gray or magenta mesh) is shown, as well as the F_0-F_c omit map (3σ, green mesh) for which HYD1 was omitted from the Fourier synthesis calculation. Note the feature marked "X" in (b), suggesting the presence of a tautomeric equilibrium as depicted in (c) for the oxidized form. Distances are in Å. The same color scheme has been used to depict the atom types and density maps in all figures: N blue, C yellow/pink, O red, D gray.

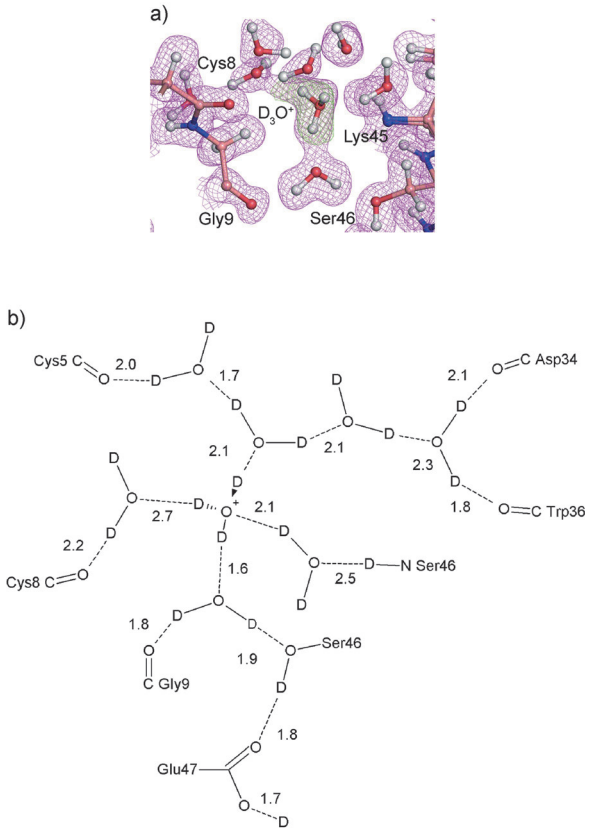

Figure 2. a) Neutron scattering density maps showing the HYD2 D_3O^+ ion in the region of Pro44–Pro19–Ser46 in the oxidized form of the protein. The $2F_0-F_c$ map (contoured at 1σ in magenta) is shown as well as the F_0-F_c omit map (3σ in green) for which the HYD2 ion was omitted from the Fourier synthesis calculation. b) Connectivity of the water and amino acid residues around the D_3O^+ ion. Distances are in Å.

having unit occupancy and with low temperature factors (see the Supporting Information). However, in the case of the oxidized structure, a clear peak (at 4.7σ level, and marked as "X" in Figure 1b) is seen located between HYD1 and the carbonyl group of Leu51. The fact that this peak is absent from the corresponding F_0-F_c X-ray maps, implies that it corresponds to a deuterium atom and not to a heavier atom that would have been detectable by X-rays, and may be part of an imidic acid tautomerization. The carbon–nitrogen bond length of the amide as seen in the X-ray analysis is 1.33 Å consistent with a normal amide bond.

A second D_3O^+ ion, designated HYD2, is found in the Pro44–Pro19–Ser46 region of both reduced and oxidized forms; the corresponding density maps for the oxidized form are shown in Figure 2. Refinement with full deuterium atom occupancy yields low temperature factors for all the atoms involved. HYD2 is located about 9.7 Å from the [Fe-S_4] cluster and forms water-mediated hydrogen bonds with residues Cys5, Cys8, and Ser46* (Ser46* is a symmetry-related monomer). The dense hydrogen-bond network centered on the D_3O^+ ion binds together nearby water molecules and protein residues, notably two cysteine residues involved in the [Fe-S_4] cluster.

A third D_3O^+ ion (HYD3) is observed in both the reduced and oxidized forms at about 9.0 Å from the [Fe-S_4] cluster near the Pro25 and Ser24 residues (Figure 3). Two of the three deuterium atoms refine with unit occupancy, but the third, which has good hydrogen bonding geometry with respect to the Ser24 hydroxy group, has a lower occupancy, as does the deuterium atom of the Ser24 hydroxy group.

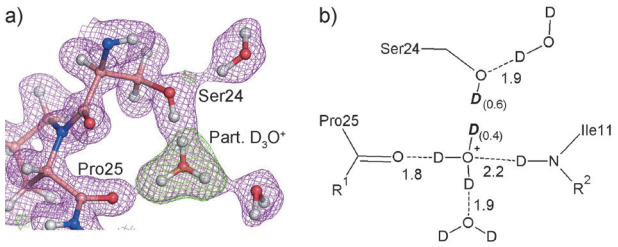

Figure 3. a) Neutron scattering density maps showing HYD3 near Ser24 in the oxidized form of the protein. The $2F_0-F_c$ map (contoured at 1σ in magenta) is shown, as well as the F_0-F_c omit map (3σ in green) for which HYD3 was omitted from the Fourier synthesis calculation. b) Connectivity of the D_3O^+ ion, including occupancies (in parentheses) for the two partially occupied deuterium atoms on HYD3 and the Ser24 hydroxy group. Occupancies are quoted to one decimal place, in line with Tanley et al.[9] Distances are in Å.

In the final refinement, the total of the two D occupancies was constrained to 1.0 for both the reduced and the oxidized structures. The refined occupancies of the shared D atom of the HYD3 D_3O^+ are 0.4 for the reduced and oxidized structures. These results suggest a proton exchange equilibrium involving the Ser24 hydroxy group and HYD3.

A fourth D_3O^+ ion (HYD4) is observed hydrogen-bonded to the Ala16 carbonyl group for both the reduced and oxidized structures (Figure 4). One of the deuterium atoms, which points into a region of disordered solvent, refines to an occupancy of 0.5 in the reduced structure, and 0.3 in the oxidized structure, again suggesting the possibility of a D_2O/D_3O^+ equilibrium involving disordered D_2O solvent.

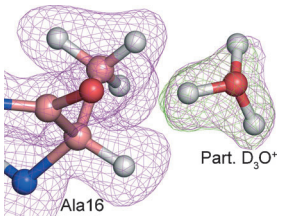

Figure 4. The HYD4 D_3O^+ ion hydrogen-bonded to Ala16 in the oxidized rubredoxin structure. The $2F_0-F_c$ map (contoured at 1σ in magenta) is shown, as well as the F_0-F_c omit map (3σ in green) for which the HYD4 ion was omitted from the structure factor calculation. A D_3O^+ ion is also found at the same position in the reduced structure.

Along with the imidic acid tautomerisation associated with HYD1/Leu51 (Figure 1), there is further evidence of protonation shifts between the reduced and oxidized rubredoxin structures. Glu47 is unprotonated in the reduced form (Figure 5a) and protonated in the oxidized form (Figure 5b).

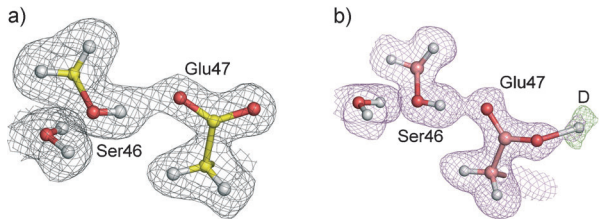

Figure 5. Neutron scattering density maps showing a protonation shift as demonstrated by the absence of a carboxylic deuterium at Glu47 in the reduced form (a), and its presence in the oxidized form (b). In each case, the $2F_0-F_c$ map (contoured at 0.7σ, gray or magenta) is shown, as well as the F_0-F_c omit map (3σ, green) for which the deuterium atom was omitted from the Fourier synthesis calculation.

This deuterium atom is an integral part of the hydrogen bond network associated with the D_3O^+ ion near Ser46 (see Figure 2), and which extends to the amine group of Lys6. It is located at about 9.6 Å from the [Fe-S_4] cluster and separated from it by a channel containing hydrophilic and hydrophobic chemical groups, but it is free of hydrogen bonds.

In the oxidized form, a protonation shift also occurs such that the carboxylic group of Asp15 is protonated (not shown). This deuterium atom lies in a solvent pocket and is close to Met0, Lys2, and the carboxyl group of Asp53.

This study is the first neutron analysis to allow the direct observation of changes involving hydrogen atoms in a redox protein system, and the results bring out some key points relevant to the redox and thermostability properties of the protein. The D_3O^+ ions are clearly involved in well-ordered hydrogen bonding networks located in the protein hydration shell,[10] and this may contribute to the exceptional thermostability of the protein. Calculations show that the Gibbs free energy for a hydrogen bond formed by donation of a hydronium hydrogen to an acceptor is much higher than for a water molecule under the same conditions.[11] Intriguingly, the more favorable hydrogen bonding energetics of a hydronium compared to water may play an important role in both the stability of rubredoxin and its redox properties. Furthermore the HYD1 (Figure 1), HYD2 (Figure 2), and HYD3 (Figure 3) D_3O^+ ions are all located at about 9 Å from the redox-active center. While this does not place them within the immediate vicinity of the rubredoxin redox center, it is known that electron tunneling and transfer processes can occur over considerable distances.[12] It is conceivable that the hydronium ions identified in this study may be implicated in such processes. The dense hydrogen bond network involving these hydronium ions in proximity to the [Fe-S_4] center may play a decisive role in the redox catalysis mechanism of the [Fe-S_4] center by favoring the approach and docking of protein partners and reactants. For example, the differences we have noted between the reduced and oxidized forms of rubredoxin are likely to be of significance for an understanding of the electron transfer processes associated with the oxidative stress mechanism that involves rubredoxin, rubredoxin oxidoreductase, rubrerythrin, and superoxide reductase.[13]

This is one of the highest-resolution room-temperature neutron crystallographic structure determinations available in the protein database, with data observed to d-spacing as small as 1.05 Å. An earlier study citing high resolution was that of crambin described by Chen et al.[14] (but with completeness of only 65% in the highest resolution shell), where data at 1.10 Å were recorded. The use of neutrons for the precise characterization of hydronium ions in proteins was recently described by Kovalevsky et al.[15] in their monochromatic study of xylose isomerase, and is highly significant for an understanding of enzymatic processes. We assert that the reason the D_3O^+ ions described in this work were not observed as such in previous neutron studies of hydrogenated and partially deuterated rubredoxin[8,16] is directly attributable to the more limited resolutions available. In truncation tests of our datasets, D_3O^+ ions were not visible as four-atom entities at resolutions poorer than circa 1.6 Å.

In summary, detailed neutron crystallographic analyses were carried out at near-atomic resolution of both reduced and oxidized forms of perdeuterated *Pyrococcus furiosus* rubredoxin, a small iron–sulfur redox protein having remarkable thermostability. Four D_3O^+ ions were identified in both oxidized and reduced forms of the structure (Figure 6): three are located close to the protein main chain and one forms part of a hydrogen bonded network with ordered solvent. One of the D_3O^+ ions is located near the main chain amide group of Leu51 and appears to be involved in a redox-driven tautomeric shift between amino and imino forms of the residue. The three other D_3O^+ groups are bound in essentially the same places in both the reduced and the oxidized forms of the protein. In two of these there is evidence of D_2O–D_3O^+ equilibria that may be important in charge transfer. In the

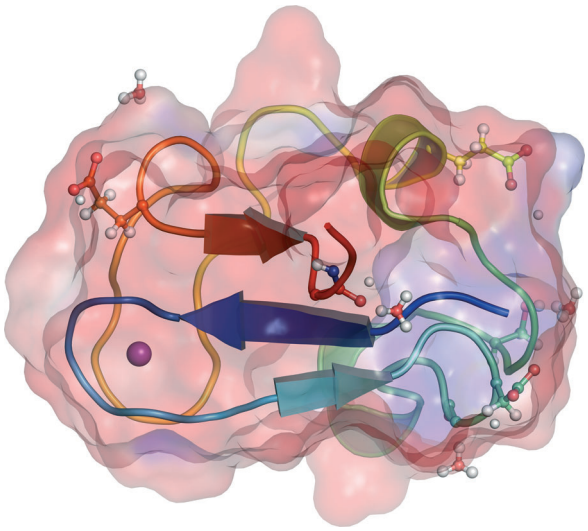

Figure 6. The overall neutron structure of the oxidized form of *Pf* rubredoxin, showing the D_3O^+ ions (red and gray molecules) and deuterium atoms (gray spheres) bound to carboxylic acid side chains. The electrostatic surface is shown (blue for positive and red for negative).

oxidized form, Asp15 and Glu47 are seen to be protonated, while Asp13 is not protonated. In contrast, in the reduced form, Asp13 is protonated and Asp15 and Glu47 are not protonated. These observations suggest that hydronium ions and their interaction with the surrounding solvent play a key role in the protonation shifts and charge transfer processes associated with the change between oxidized and reduced forms of the protein. They also demonstrate the power of high-resolution neutron crystallography, used in conjunction with perdeuterated protein, to image these vital details of protein structure.

Received: August 31, 2012
Published online: December 6, 2012

Keywords: neutron crystallography · protein perdeuteration · protonation states · rubredoxin · X-ray diffraction

[1] L. C. Sieker, R. E. Stenkamp, J. LeGall, *Methods Enzymol.* **1994**, *243*, 203 – 216.
[2] a) J. Wastl, H. Sticht, U. G. Maier, P. Rosch, S. Hoffmann, *FEBS Lett.* **2000**, *471*, 191 – 196; b) S. Zauner, M. Fraunholz, J. Wastl, S. Penny, M. Beaton, T. Cavalier-Smith, U. G. Maier, S. Douglas, *Proc. Natl. Acad. Sci. USA* **2000**, *97*, 200 – 205.
[3] K. Ma, M. W. Adams, *J. Bacteriol.* **1999**, *181*, 5530 – 5533.
[4] R. Hiller, Z. H. Zhou, M. W. Adams, S. W. Englander, *Proc. Natl. Acad. Sci. USA* **1997**, *94*, 11329 – 11332.
[5] R. Bau, *J. Synchrotron Radiat.* **2004**, *11*, 76 – 79.
[6] M. P. Blakeley, *Crystallogr. Rev.* **2009**, *15*, 157 – 218.
[7] K. Kurihara, I. Tanaka, T. Chatake, M. W. Adams, F. E. Jenney, Jr., N. Moiseeva, R. Bau, N. Niimura, *Proc. Natl. Acad. Sci. USA* **2004**, *101*, 11215 – 11220.
[8] A. S. Gardberg, A. R. Del Castillo, K. L. Weiss, F. Meilleur, M. P. Blakeley, D. A. Myles, *Acta Crystallogr. Sect. D* **2010**, *66*, 558 – 567.
[9] S. W. Tanley, A. M. Schreurs, L. M. Kroon-Batenburg, J. Meredith, R. Prendergast, D. Walsh, P. Bryant, C. Levy, J. R. Helliwell, *Acta Crystallogr. Sect. D* **2012**, *68*, 601 – 612.
[10] M. W. Day, B. T. Hsu, L. Joshua-Tor, J. B. Park, Z. H. Zhou, M. W. Adams, D. C. Rees, *Protein Sci.* **1992**, *1*, 1494 – 1507.
[11] O. Markovitch, N. Agmon, *J. Phys. Chem. A* **2007**, *111*, 2253 – 2256.
[12] J. R. Winkler, *Curr. Opin. Chem. Biol.* **2000**, *4*, 192 – 198.
[13] M. V. Weinberg, F. E. Jenney, Jr., X. Cui, M. W. Adams, *J. Bacteriol.* **2004**, *186*, 7888 – 7895.
[14] J. C. Chen, Z. Fisher, A. Y. Kovalevsky, M. Mustyakimov, B. L. Hanson, V. V. Zhurov, P. Langan, *Acta Crystallogr. Sect. F* **2012**, *68*, 119 – 123.
[15] A. Y. Kovalevsky, B. L. Hanson, S. A. Mason, T. Yoshida, S. Z. Fisher, M. Mustyakimov, V. T. Forsyth, M. P. Blakeley, D. A. Keen, P. Langan, *Angew. Chem.* **2011**, *123*, 7662 – 7665; *Angew. Chem. Int. Ed.* **2011**, *50*, 7520 – 7523.
[16] a) T. Chatake, K. Kurihara, I. Tanaka, I. Tsyba, R. Bau, F. E. Jenney, Jr., M. W. Adams, N. Niimura, *Acta Crystallogr. Sect. D* **2004**, *60*, 1364 – 1373; b) P. Munshi, S. L. Chung, M. P. Blakeley, K. L. Weiss, D. A. Myles, F. Meilleur, *Acta Crystallogr. Sect. D* **2012**, *68*, 35 – 41.

